

Physico-chemical characterization and mass closure of size-segregated atmospheric aerosols in Hyytiälä, Finland

Sanna Saarikoski¹⁾, Timo Mäkelä¹⁾, Risto Hillamo¹⁾, Pasi P. Aalto²⁾, Veli-Matti Kerminen¹⁾ and Markku Kulmala²⁾

¹⁾ Finnish Meteorological Institute, Research and Development, Erik Palmenin Aukio 1, P.O. Box 503, FI-00101 Helsinki, Finland

²⁾ Department of Physical Sciences, FI-00014 University of Helsinki, Finland

Saarikoski, S., Mäkelä, T., Hillamo, R., Aalto, P. P., Kerminen, V.-M. & Kulmala, M. 2005: Physico-chemical characterization and mass closure of size-segregated atmospheric aerosols in Hyytiälä, Finland. *Boreal Env. Res.* 10: 385–400.

A size-segregated chemical composition of atmospheric aerosols was investigated in May 2004 at the SMEAR II station, southern Finland. Aerosols were collected using two 12-stage low pressure impactors (SDI) and two virtual impactors (VI). The samples were analyzed for mass, inorganic ions and organic (OC) and elemental carbon (EC). By comparing the gravimetric mass and the results from the chemical analyses, a chemical mass closure was constructed. In addition to the impactors an Electrical Low Pressure Impactor (ELPI), Differential Mobility Particle Sizer (DMPS) and Aerodynamic Particle Sizer (APS) were used to measure the mass size distribution continuously. The chemical composition of fine particles (particle diameter < 1 μm) was very similar over the whole measurement campaign with 40% of mass composed of ammonium sulfate, 35% of OC and 5% of EC. In the submicron range the chemical mass closure of the collected samples was reached within a few percent on average. The chemical mass to gravimetric mass ratio was 0.98 ± 0.10 and 1.05 ± 0.13 (average \pm S.D.) for the VI and SDI, respectively. Also, quite a good agreement was obtained between the mass size distributions measured with the ELPI and that measured with the DMPS-APS combination. When the total mass concentration of the fine particles was calculated, the mass concentration of the ELPI was found to be larger than that of the SDI and VI (ELPI/VI ratio 1.11 ± 0.13). This may be due to the semivolatile components lost in impactors. For the SDI and DMPS-APS the concentration of the fine particles was smaller than that of the VI with the SDI/VI and DMPS-APS/VI ratios of 0.70 ± 0.11 and 0.92 ± 0.08 , respectively. For the DMPS and APS the mass concentration was calculated from the number concentration by estimating the particle density. The particle density was assessed in two ways; from the chemical composition of the particles (composite density) and by comparing the mass obtained from the DMPS-APS combination with the VI mass concentration (gravimetric density). The densities obtained for fine particles were 1.49 ± 0.03 and 1.66 ± 0.13 g cm^{-3} for the composite and gravimetric density, respectively.

Introduction

Quantifying the climate and other effects of atmospheric aerosols is not possible without detailed information on the aerosol chemical composition as a function of the size. Over the years, a number of efforts have been made to determine the chemical composition of atmospheric aerosols and to achieve a mass closure on the chemical species for the whole mass of aerosols collected at a variety of urban and rural sites (Chow *et al.* 1994, Putaud *et al.* 2000, Puxbaum *et al.* 2000, Salma *et al.* 2001, Lonati *et al.* 2005). However, in most of the studies only fine and coarse particles have been analyzed separately. Few studies have been focused on a more detailed size-resolved mass closure (eg. Nuesüß *et al.* 2000, Matta *et al.* 2003, Sellegri *et al.* 2003, Putaud *et al.* 2004).

Until recently, the elucidation of the organic fraction of the aerosol has been the most difficult task in achieving the chemical mass closure. The inorganic and elemental fractions of the particle mass have been characterized well, while little is known about the composition of the organic fraction. Organic matter (OM) can constitute up to 70% of the fine aerosol mass (Tolocka *et al.* 2001), but only 10%–40% of it can be usually attributed to specific compounds (Rogge *et al.* 1993, Fraser *et al.* 2002, Radzi Bin Abas *et al.* 2004).

In this work the mass closure was studied from two perspectives. Firstly, a chemical mass closure was constructed for size-segregated impactor samples by extensive chemical analyses, in which ions were measured with ion chromatography and organic carbon (OC) and elemental carbon (EC) with thermal-optical transmission (TOT) method. Secondly, a closure between several instruments was studied by comparing the mass concentrations of the impactors to those based on the instruments measuring aerosol size distributions continuously. In case of the continuous measurements, the size-segregated mass was obtained from the instrument basic data using the algorithm provided by the manufacturer (Electrical Low Pressure Impactor, ELPI) or calculated from the number size distribution (Differential Mobility Particle Sizer, DMPS and Aerodynamic Particle Sizer, APS).

Aerosol measurements were carried out at the SMEAR II station in Hyytiälä, Finland, in May 2004. Hyytiälä is known as a site where particle growth events have been observed and studied extensively (Mäkelä *et al.* 1997, Kulmala *et al.* 2001). During the measurement period considered here, several nucleation events were detected. This enabled a comparison of the chemical composition of the nucleation event samples to the non-event samples. The focus of this study was mainly on the fine size range (particle diameter < 1 µm), and data on coarse particles present only supplementary information.

Materials and methods

Description of the site and instruments

The aerosol measurements were made in Hyytiälä (61°51'N, 24°17'E, 181 m a.s.l.) at the SMEAR II station between 7 and 31 May 2004. The field station is located in the boreal forest and represents background area of southern Finland. The measurement site is discussed in detail in Kulmala *et al.* (2001). Briefly, the field station is dedicated to studies on the relationship of atmosphere and forest in boreal climate zone. At the SMEAR II station continuous gas and particle measurements as well as intensive campaigns are performed.

During the field measurements of this study the mass concentrations were very small. Therefore, to get enough mass for the impactor samples, a sampling period of two days was chosen. The number of two-day samplings was eight, in addition to which one three-day and one five-day sampling was performed. The aerosol samples were collected using two Small Deposit area low pressure Impactors (SDI) and two virtual impactors (VI) in parallel. The SDI and the VI have been described in detail elsewhere (Maenhaut *et al.* 1996, Loo and Cork 1988). In short, the SDI is a 12-stage, low-pressure, multinozzle inertial impactor that operates at a flow rate of 11 l min⁻¹. The nozzles of the impactor stages are spaced closely together so that the diameter of aerosol deposition area remains smaller than 8 mm for each stage. The aerodynamic cutoff diameters of the stages are 0.045, 0.088, 0.142, 0.235, 0.380,

0.580, 0.800, 1.06, 1.61, 2.60, 4.07 and 8.40 μm . The VI is a modified version of the original design of Loo and Cork (1988), which divides particles into two size fractions using 2.5 μm cut-off diameter. The modified VI used in this work divides particles into two size fractions: fine (particle aerodynamic diameter $D_a < 1.3 \mu\text{m}$) and coarse particles ($1.3 \mu\text{m} < D_a < 10 \mu\text{m}$). The lower cut-off diameter of the VI enables more accurate comparison of the aerosol mass concentration with the instruments measuring the submicron fraction only (Putaud *et al.* 2000). The flow rate of the VI is 16.7 l min^{-1} .

One SDI and VI, termed here AI-SDI and T-VI, were used to collect particles for mass and ion analyses. For this purpose, either Apiezon L-greased aluminum substrates (AI-SDI) or Teflon filters (T-VI) (Millipore Fluoropore; pore size 3.0 μm ; diameter 47 mm) were used. The other SDI and VI (Q-SDI and Q-VI) were used to collect OC and EC on quartz fiber filters (Whatman QMA, diameter 47 mm). In the Q-VI, a second quartz filter (back-up filter) was placed behind the first one to collect the particulate material evaporated from the front filter.

Quartz material is very porous and the surface of the filter is rough. When porous substrates are used in cascade impactors (the SDI in this study), the shape of the collection efficiency curves changes and the cut-points shift (Sillanpää *et al.* 2003, Marjamäki and Keskinen 2004). Therefore, the behavior of the quartz substrates in the cascade impactors needs to be studied in more detail before reliable carbonaceous matter size distributions are obtained. In this study, however, because the new calibration is not yet available the quartz substrates were assumed to behave similarly to the non-porous and flat substrates in order to construct the chemical mass closure.

In addition to aerosol particles, quartz material collects an unknown fraction of gaseous organic compounds (Turpin *et al.* 2000). To reduce this positive artifact, gas-phase organic compounds were removed from the air stream before the Q-SDI and Q-VI with three multi-annular denuders (URG-2000, $30 \times 242 \text{ mm}$, Chapel Hill, NC). The denuders were coated with XAD-4 (polystyrene-divinylbenzene) adsorbent according to Gundel *et al.* (1995). The denuders were changed

every day to avoid the overloading. After use the collected gas-phase compounds were extracted from the adsorbent with acetonitrile and hexane. The extract of the denuders was not analyzed in this work. The denuders were recoated after ten days of use.

The physical characterization of aerosols was performed with a DMPS, APS and ELPI. The DMPS system consisted of two parallel DMPS devices: one classifying particles between 3 and 10 nm and the other between 10 and 500 nm (mobility diameter). Both instruments used a Hauke-type differential mobility analyzer (DMA) (Winklmayr *et al.* 1991) and a closed loop sheath flow arrangement (Jokinen and Mäkelä 1997). The CPCs used were TSI Model 3025 and TSI Model 3010, respectively. For larger particles the APS (TSI Model 3320) was used. The APS measured the number size distribution from 0.5 μm to 20 μm (aerodynamic diameter). The size range of the ELPI (Outdoor Air ELPI, manufactured by Dekati Ltd., Tampere, Finland) was from 29 nm to 10 μm (aerodynamic diameter). In this work, however, the size range of the ELPI was extended to particles below 29 nm by adding an electrical filter stage (ELA 650). Prior to the ELPI, there was a conditioning unit (The Dekati Ambient Sampler, DAS 3100) where sample aerosol was first heated up to 30 °C and then led through a Nafion drier. The ELPI was used only in an electrical mode, so that the impactor substrates were analyzed neither gravimetrically nor chemically. The time resolution of the ELPI and APS was one second and one minute, respectively, but the data were averaged over ten minutes to make the data handling easier. The time resolution of the DMPS was ten minutes.

Sample handling, weighing and chemical analyses

The AI-SDI and the T-VI samples were pre- and post-weighed using a Mettler microbalance (MT5, Mettler-Toledo Inc. Hightstown, NJ). The readability of the balance was 1 μg , precision $\pm 4 \mu\text{g}$ corresponding to PM_{10} mass concentration uncertainty of ± 0.32 and $\pm 0.09 \mu\text{g m}^{-3}$ for SDI and VI, respectively. After the weighing, the samples were stored in a refrigerator in plastic

test tubes (AI-SDI samples) or Petrislides (T-VI samples).

The AI-SDI and T-VI samples were analyzed chemically for water-soluble ions. First, the samples were wetted with 0.5 ml of methanol and 4.5 ml of deionized water (Millipore Alpha-Q, resistance 18.2 Ω) was added. The test tubes were then rotated for ten minutes, after which the anions and cations were analyzed simultaneously using two Dionex-500 ion chromatography systems. An AS11 analytical column with an AG11 guard column was used for anions and a CS12A analytical column with a CG12A guard column was used for cations. Chemical suppression with sulfuric acid and an electrochemical suppression were used for anions and cations, respectively. The eluents were 2.5–29 mM NaOH solution for anions (gradient) and 20 mM methanesulfonic acid for cations (isocratic elution). Injection of the samples was done manually using either a 1000- μ l loop (anions) or a 300- μ l loop (cations). The analyzed ions were Na⁺, NH₄⁺, K⁺, Mg²⁺, Ca²⁺, SO₄²⁻, NO₃⁻, Cl⁻, methanesulfonate (MSA⁻) and oxalate (Ox²⁻). The uncertainty of ion analyses was estimated to be 5%–10% (Teinilä *et al.* 2000).

The Q-SDI and Q-VI samples were stored in a refrigerator after the sampling and analyzed for OC and EC with the thermal-optical transmission method using a carbon analyser developed by Sunset Laboratory Inc., Oregon. A 1.5-cm² sample piece was punched from the VI sample, while the SDI samples were analyzed as a whole. The thermal method used in this study was similar to the method of Viidanoja *et al.* (2002). In short, the thermal method had two distinct phases to differentiate between OC and EC. During the first phase the sample was kept in

helium atmosphere and heated in four steps; 310, 480, 615 and 800 °C. In the original method the last step was 900 °C, but in this study the temperature was reduced to 800 °C in order to avoid the evolution of EC in the first phase. In the helium phase volatile organic compounds were measured. The second phase, the oxygen phase, had four consecutive temperature steps as well (675, 750, 825 and 920 °C). In the oxygen phase EC and pyrolysed OC were determined.

In the SDI, particles are impacted into 1–50 deposits depending on the impactor stage. Since the SDI sample is unhomogeneous, the optical pyrolysis correction of the instrument is not valid for the SDI samples. Here pyrolytic OC in the Q-SDI samples was calculated with the help of measured pyrolytic OC in the parallel VI samples (Viidanoja *et al.* 2002). Due to the small OC and EC concentrations the uncertainties in the OC and EC analyses were estimated to be 15 and 40%, respectively, in this study. The instruments used and the analyses performed for the impactor samples are listed in Table 1.

Other measurements and data processing

Temperature, relative humidity, wind speed and wind direction data were recorded at the SMEAR II station. The meteorological data were averaged to thirty minutes which was sufficient for the sampling period of two days or more. In order to identify the origin and the transport routes of the measured air masses, 120-hour backward trajectories were calculated for every sampling period (FLEXTRA, Stohl and Wotawa 1995).

Table 1. The instruments, size ranges, number of channels/stages, time resolutions and analyses in the field campaign in Hyytiälä.

Instrument	Size range	Number of channels/stages	Time resolution	Analyses
DMPS	0.003–0.5 μ m ^a	32	10 min	
APS	0.5–20 μ m ^b	52	1 min	
ELPI	< 0.029–10 μ m ^b	12	1 sec	
AI-SDI	0.045–10 μ m ^b	12	2 days	mass, ions
Q-SDI	0.045–10 μ m ^b	12	2 days	OC, EC
T-VI	< 10 μ m ^b	2	2 days	mass, ions
Q-VI	< 10 μ m ^b	2	2 days	OC, EC

^a electrical mobility diameter, ^b aerodynamic diameter.

The SDI, VI, APS and ELPI measured the aerodynamic particle diameter (D_a), while the DMPS measured the electrical mobility diameter (D_b). The relation between these two quantities is (Hinds 1999):

$$\frac{D_a}{D_b} = \left(\frac{C_c(D_b)}{C_c(D_a)} \right)^{1/2} \left(\frac{\rho_p}{\rho_0} \right)^{1/2},$$

where $C_c(D)$ is a slip correction factor for a particle of diameter D , ρ_0 is the unit density (1 g cm^{-3}) and ρ_p is the particle density.

The DMPS and the APS measured the particle number size distribution $n_N(D_a)$ which was transformed to particle mass size distribution $n_M(D_a)$ using the following equation (Seinfeld and Pandis 1998):

$$n_M(D_a) = \rho_p \frac{\pi}{6} D_b(D_a)^3 n_N(D_a).$$

Here $n_N(D_a)$ is given in units cm^{-3} and $n_M(D_a)$ in units $\mu\text{g m}^{-3}$.

Results and discussion

General features of the measurement campaign

Meteorological parameters and the concentrations of mass and major components in the fine

fraction (PM_{10}) are given separately for each sampling period in Table 2. The concentrations were measured with the VI. In two samplings (11–16 May 2004 and 28–31 May 2004), OC and EC were not analyzed due to the absence of the denuders in the sampling line. In the beginning of the measurement campaign the air masses came from the south-east and the concentrations were remarkably large. During the second sampling period the air masses originated first from the east and after that from the north-east, and the concentrations were significantly smaller as compared with those during the first sampling. After these two periods less polluted air originating from the North Atlantic and Arctic Ocean was encountered.

During the measurement campaign, the fine particle mass concentration ranged from 1.1 to $16.1 \mu\text{g m}^{-3}$ (Table 2). Even when the air masses came from different areas and the mass concentrations varied significantly, the chemical composition of fine particles was quite similar over the whole campaign. The most prominent components in fine particles were OC, sulfate, ammonium and EC. On average, 30% of the fine particle mass was comprised of sulfate, 35% of OC, 9% of ammonium, 5% of EC and 2% of MSA. For all the other analyzed components the individual contribution to fine particles was smaller than 1%. The mass ratio of ammonium to non-sea salt sulfate, calculated from the measured sulfate, sodium and standard sea water

Table 2. Temperature, relative humidity and wind speed (average \pm S.D.), prevailing wind direction and PM_{10} concentrations for mass, ions, OC and EC.

Measurement period	Weather parameters			PM_{10} concentrations (VI) $\mu\text{g m}^{-3}$				
	T ($^{\circ}\text{C}$)	RH (%)	Wind speed (m s^{-1}) and direction	Mass	SO_4^{2-}	NH_4^+	OC	EC
7–9 May 2004	17.4 ± 3.7	48 ± 16	1.6 ± 0.7 east	16.1	4.56	1.63	5.06	0.52
9–11 May 2004	8.7 ± 6.3	71 ± 16	2.5 ± 0.4 north	6.31	1.94	0.67	2.11	0.16
11–16 May 2004	3.7 ± 2.5	57 ± 20	1.9 ± 0.7 north	2.36	0.96	0.06	–	–
16–18 May 2004	7.1 ± 3.4	47 ± 15	2.6 ± 0.8 west	2.41	0.75	0.27	0.73	0.10
18–20 May 2004	6.3 ± 2.4	81 ± 13	2.6 ± 0.8 south-west	1.78	0.47	0.16	0.92	0.10
20–22 May 2004	5.7 ± 2.3	75 ± 16	2.5 ± 0.8 west	1.53	0.43	0.16	0.46	0.08
22–24 May 2004	5.6 ± 2.4	74 ± 16	1.9 ± 1.1 north-west	1.14	0.34	0.12	0.40	0.10
24–26 May 2004	8.3 ± 2.8	63 ± 19	1.6 ± 0.5 north	2.77	0.85	0.27	0.88	0.16
26–28 May 2004	8.6 ± 2.2	69 ± 10	2.2 ± 0.8 north	3.39	1.13	0.31	1.16	0.14
28–31 May 2004	7.8 ± 2.7	72 ± 14	2.0 ± 1.0 west	1.52	0.29	0.09	–	–

– not measured.

composition (Brewer 1975) varied in the range 0.31–0.37 with an average of 0.35. This ratio is close to the value of 0.38 corresponding to the ammonium sulfate mixture, which means that almost all ammonium and sulfate were in the form of ammonium sulfate. Of the total amount of ions analyzed, 95% was made of ammonium sulfate.

The size-segregated chemical composition of the particles was measured with the SDI. The mass size distribution of ammonium sulfate was unimodal with an accumulation mode peaking at 0.3–0.5 μm . The mass size distributions of OC and EC are not discussed here because of the uncertainty caused by the fact that the impactor was not calibrated for quartz fiber substrates. The size distributions of the mass and sulfate measured with the SDI will be discussed more in later sections.

In order to investigate the potential experimental uncertainties in the impactor samplings, the SDI to VI concentration ratios were calculated for the mass, ions, OC and EC for all the parallel SDI and VI samplings. The fine particle concentration of the SDI was obtained by summing up the seven lowest stages ($D_a < 1.06 \mu\text{m}$), after which the fine concentration of the SDI was compared to the fine concentration of the VI

($D_a < 1.3 \mu\text{m}$). On average, the SDI to VI concentration ratios were 0.70, 0.72, 0.67, 0.78 and 0.84 for mass, sulfate, ammonium, OC and EC, respectively. The systematic difference between the SDI and the VI was caused most likely by bouncing and inter-stage losses of particles in the SDI. This assumption is supported by the fact that the SDI to VI ratios were smaller for ions and mass, collected on aluminum substrates, than they were for OC and EC which were collected on the porous substrates that reduced the bounce-off.

Chemical mass closure of size-segregated aerosols

The chemical mass closure was studied by comparing the mass derived from the chemical analyses to the gravimetric mass obtained by weighing the samples. The mass of chemical components was calculated by summing up EC, OM and all ions, except MSA^- and Ox^{2-} which are included in OM, for each impactor stage separately. The size-segregated mass closure was calculated for eight samples excluding the samples with no OC and EC results.

The mass closure requires the conversion

Table 3. Uncertainties (%) in the gravimetric and chemical mass and the relative uncertainties $S(x)/x_i$ in the parameters associated with the chemical mass (sulfate, ammonium, OM, EC). Relative uncertainties are combined according to the law of propagation of errors to assess the overall uncertainty in chemical mass.

Stage	Gravimetric mass	Sulfate	Ammonium	OM	EC	Chemical mass
1	±418	±8	±16	–35, +63	±50	–27, +55
2	±104	±7	±11	–35, +65	±48	–19, +51
3	±46	±7	±11	–34, +69	±41	–18, +51
4	±42	±7	±11	–34, +71	±40	–15, +48
5	±38	±7	±11	–34, +71	±40	–16, +49
6	±84	±7	±11	–34, +69	±41	–19, +52
7	±70	±7	±12	–34, +66	±42	–22, +53
8	±64	±8	±15	–35, +64	±43	–24, +53
9	±167	±10	±26	–35, +64	±45	–28, +56
10	±31	±9	±28	–34, +66	±42	–27, +55
11	±32	±9	±26	–34, +67	±42	–27, +56
12	±279	±33	±753	–41, +58	±52	–35, +51
Fine	±4	±5	±11	–20, +49	±22	–11, +26

Uncertainty parameters included in the calculations are uncertainty in analyses (weighing for gravimetric mass), variability in blanks, uncertainty in sampling air volume and uncertainty in molecular/carbon correction factor (only for OM).

of the mass of organic carbon to that of organic matter. There is no instrument to measure this value directly. Turpin *et al.* (2001) recommended the conversion factor of 2.1 ± 0.2 for a non-urban aerosol, but the limitation of that estimate is that less than 20% of OM was identified in the chemical analysis. Another promising technique to measure the conversion factor is the Fourier Transform Infrared spectroscopy, which quantifies OM by functional groups rather than by individual compounds. Russel (2003) used this technique for the samples collected in the Caribbean and northeastern Asia and obtained a conversion factor of just below 1.4. In this work a factor of 1.4 was chosen. The uncertainty of the conversion factor ($-0.2, 0.7$) has been included in the uncertainty calculations of OM (Appendix and Table 3). The average overall uncertainty of OM was -35% and 66% for individual SDI stage and -20% and 49% for the VI. The uncertainties were calculated using the procedure of error propagation described by Putaud *et al.* (2000).

Generally, the agreement between the chemical mass and the gravimetric mass was good. The ratio between the chemical and gravimetric mass for the fine particles was in the range 0.87–1.19 with an average of 0.98 for the VI. For the SDI the corresponding ratio was slightly poorer with the range of 0.88–1.24 and an average of 1.05. The ratio above unity for the SDI samples was obviously due to the more efficient collection of OC and EC using quartz substrates as compared with the collection of mass using aluminum substrates, as well as due to uncertainties involved in weighing the substrates with a remarkably small mass. The estimated uncertainty in weighing the SDI substrates with a small mass loading could be even larger than $\pm 50\%$ for individual stages (Table 3). As a result, the size-segregated mass closure was more sensitive to uncertainties in weighing the SDI samples than to uncertainties in chemical analyses. The uncertainties associated with the chemical mass closure are presented in detail in the Appendix and Table 3. The extent of mass closure presented here is comparable to that obtained in the other studies, where the size-segregated mass closure has been reached within a few percent in the submicron range (Neusüß *et al.* 2000, Matta *et al.* 2003, Putaud *et al.* 2004).

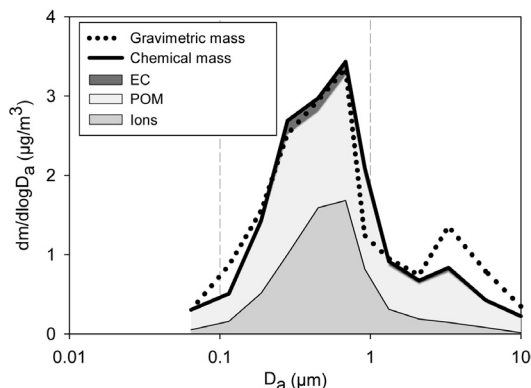


Fig. 1. Size-segregated mass closure for the period 26–28 May 2004 in Hyytiälä. The concentrations are plotted as a function of the geometric mean of the stage boundary (cut-off) diameters.

There was no unexplained mass in the accumulation mode size range. In spite of the fact that the relative humidity of the weighing room was not measured, the water content of particles was expected to be small and the amount of water associated with particles was not taken into account when constructing the mass closure. In literature the aerosol water content has been assessed in different ways. Sellegri *et al.* (2003) applied a growth factor of 1.02 for submicron particles, which led to a mass of water that was approximately 3% of the total mass. However, Harrison *et al.* (2003) suggested a factor of 1.38 for ammonium sulfate when the samples were weighed at a relative humidity of 45%–55%. In this study, the use of the factor of 1.38 for ammonium sulfate would have meant that 15% of mass would have been made of water, which undoubtedly would have been too much. However, the fact that the SDI was classifying the particles at ambient relative humidity affected the modal parameters of the aerosol size distribution. This will be discussed later.

An example of the size-segregated mass closure in Hyytiälä is presented in Fig. 1. In this section only the selected sample is discussed, but the general features of the mass closure were similar in all cases independent of the degree of pollution. The gravimetric mass size distribution followed closely the size distribution of chemical mass in the accumulation mode size range (Fig. 1). At around $0.1 \mu\text{m}$, the chemical mass was smaller than the gravimetric mass, whereas the

opposite was true at around 1 μm . This difference can be explained by the uncertainty in the mass size distributions of OC and EC because the SDI was not calibrated with the quartz fiber substrates. Changing the non-porous, flat substrate to the porous one will change the shape of the collection efficiency curve and shift the cut-point towards smaller particle size (Sillanpää *et al.* 2003, Marjamäki *et al.* 2004). The compatibility between chemical and gravimetric mass was poorer in the coarse mode size range. The most plausible explanation to this is that the crustal elements (Al, Fe, etc.), found mainly in the coarse size range (Pakkanen *et al.* 2001), were not analyzed here. Also, the maximum of the accumulation mode (particle diameter 0.5 μm) approximately half of the mass was composed of ions and the other half was made of OM (Fig. 1). In the smaller particle sizes (< 0.3 μm) the fraction of ions was smaller than the fraction of OM. In the lowest stage of the SDI almost 80% of mass was made of OM. This finding is in agreement with that of Temesi *et al.* (2001), who observed that in the fine size range the carbon/sulfate ratio increases with decreasing particle size.

The information about the chemical composition of particles was used to assess their density. The composite density was calculated from the bulk densities of the major constituents accord-

ing to the procedure presented by McMurry *et al.* (2002). The densities used were 1.77 g cm^{-3} for ammonium sulfate, 1.2 g cm^{-3} for OM (Turpin *et al.* 2001) and 2.0 g cm^{-3} for EC (McMurry *et al.* 2002). In this work the calculated density for fine particles varied in the range 1.42–1.51 g cm^{-3} (average 1.49 g cm^{-3}) for the VI (shown in Table 4) and 1.43–1.51 g cm^{-3} (average 1.47 g cm^{-3}) for the SDI. These calculated densities agree well with the results obtained by Stein *et al.* (1994) (composite density 1.48 g cm^{-3}). However, in the study of Stein *et al.* (1994) the composite density was significantly smaller as compared with that of the physical measurements which gave the density of 1.60–1.79 g cm^{-3} for a background environment. Composite densities derived for the SDI stages 1–7 are shown in Fig. 2. The density for the lowest two stages is small due to large fraction of organic matter in particle mass, whereas at the particle size 0.5 μm the composite density is dominated by the density of ammonium sulfate.

PM₁ mass concentrations

In addition to the chemical mass closure one of the aims of this study was to compare the PM₁ mass concentrations measured with impactors to those obtained from instruments which are measuring the size distribution continuously. The PM₁ concentrations were calculated for the VI, SDI, ELPI and DMPS-APS combination. For the VI, the fine particle concentration ($D_a < 1.3 \mu\text{m}$) was used as a PM₁ concentration, while for the SDI the seven lowest stages were summed up ($D_a < 1.06 \mu\text{m}$) and for the ELPI the filter stage plus seven lowest stages were added up ($D_a < 0.963 \mu\text{m}$) to obtain the PM₁ mass concentration. For the DMPS and APS the mass concentration was calculated from the number concentration. However, in order to obtain the mass concentration for the DMPS and APS, the density of particles needed to be known. In the previous section the composite densities of 1.49 g cm^{-3} and 1.47 g cm^{-3} were calculated for the VI and SDI, respectively, from the chemical composition of the particles. Therefore, the density of 1.5 g cm^{-3} was used to calculate the fine concentration ($D_a < 1.3 \mu\text{m}$) for the DMPS-APS. For the DMPS-APS the

Table 4. Composite and gravimetric density for the PM₁ particles.

Measurement period	Density g cm^{-3}	
	Composite ^a	Gravimetric ^b
7–9 May 2004	1.49	1.55
9–11 May 2004	1.48	1.54
11–16 May 2004	–	1.51
16–18 May 2004	1.51	1.71
18–20 May 2004	1.42	1.42
20–22 May 2004	1.50	1.78
22–24 May 2004	1.51	1.94
24–26 May 2004	1.50	1.67
26–28 May 2004	1.49	1.90
28–31 May 2004	–	1.57

^a calculated using the following densities: ammonium sulfate: 1.77 g cm^{-3} , OM: 1.2 g cm^{-3} and EC: 2.0 g cm^{-3} .

^b based on comparing the PM₁ mass concentration of the DMPS-APS and VI.

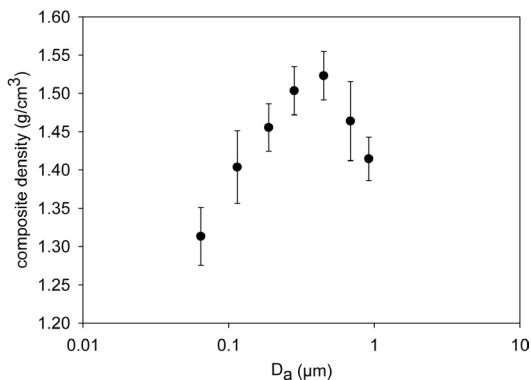


Fig. 2. Composite densities derived for individual impactor stages in fine fraction. Average densities with standard deviations are presented as a function of the geometric mean of the stage.

results from the DMPS were used up to $0.67 \mu\text{m}$ (D_a) while the results from the APS were used in the range $0.67\text{--}1.3 \mu\text{m}$ (D_a). The cut-off size of $1.3 \mu\text{m}$ was chosen for the DMPS-APS, because that was the cut-off size of the VI, considered as a reference instrument. The VI was selected for the reference of the PM_{10} mass concentration because in that method the PM_{10} mass was collected on a single filter which minimizes the experimental error. In order to compare the PM_{10} mass concentrations of different instruments, the ELPI and DMPS-APS data were averaged over the sampling period of the SDI and VI.

The PM_{10} concentrations during the measurement periods are presented in Fig. 3. It can be seen that all the instruments follow a similar trend with only minor differences. The concentration of the SDI was smaller than that of the VI, the average SDI to VI ratio of PM_{10} being equal to 0.70 ± 0.11 (average \pm S.D.) indicative of bouncing and inter-stage losses of particles in the SDI as mentioned earlier. In contrast, the ELPI to VI ratio of PM_{10} was above unity with an average of 1.11 ± 0.13 . The mass concentration of the ELPI might be larger than that of the VI because the ELPI measures also semivolatile compounds which may have been lost in impactors. In this work the mass concentration ratio between the ELPI and VI was closer to unity as compared with the results of Hitzengerger *et al.* (2004), who observed that the $\text{PM}_{2.5}$ concentration of the ELPI was nearly twice that of the filter sampling. Besides the different cut-off size, particles were

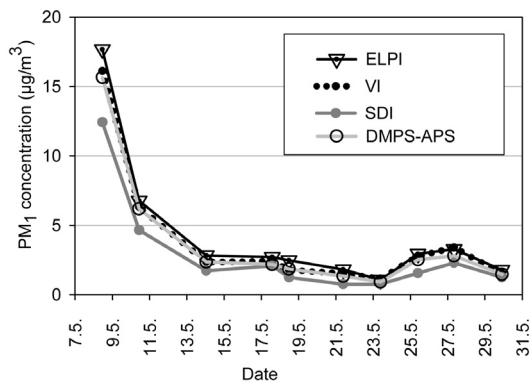


Fig. 3. PM_{10} concentrations measured with the ELPI, VI, SDI and DMPS-APS in Hyttiälä.

measured at different relative humidity in this study compared to the study of Hitzengerger *et al.* (2004). In this study the ELPI was used with a drier, whereas Hitzengerger *et al.* (2004) measured at ambient relative humidity.

The PM_{10} concentration of the DMPS-APS was slightly smaller than that of the VI, the average being equal to 0.92 ± 0.08 . The difference between the DMPS-APS and VI concentrations can be explained by the fact that the density of the particles must be estimated. The density used for the DMPS-APS was 1.5 g cm^{-3} but, as the results revealed, the actual density might be larger than that assumed. In order to assess the density of the particles in a different way, the PM_{10} mass concentration of the DMPS-APS was set to equal the concentration of the VI, after which the new value of the density was obtained for each sample ($n = 10$). This density, called the gravimetric density, ranged from 1.42 to 1.94 g cm^{-3} averaging 1.66 g cm^{-3} (Table 4). Compared with the composite density, the gravimetric density was closer to the value measured in a background environment (Stein *et al.* 1994; $1.60\text{--}1.79 \text{ g cm}^{-3}$). The gravimetric density will be used in the subsequent section in addition to the composite density.

Mass size distribution of the SDI, ELPI and DMPS-APS

The PM_{10} mass was investigated in more detail by constructing the mass size distributions for the

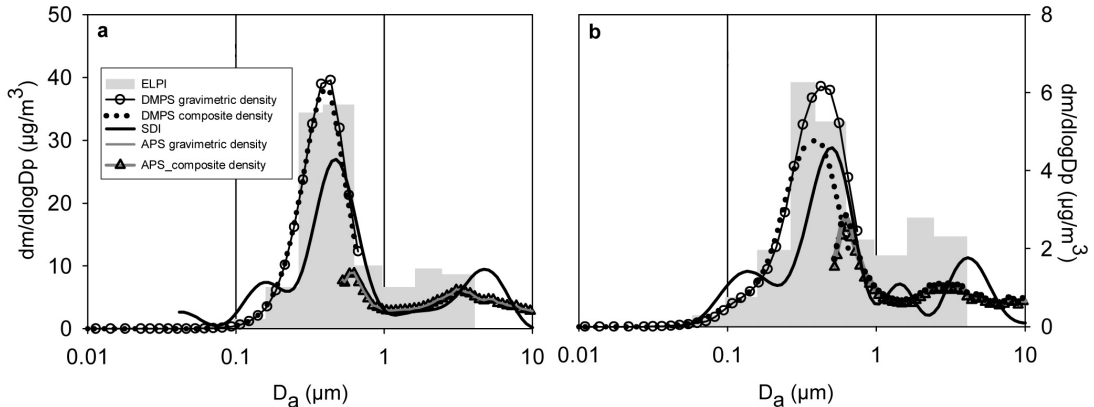


Fig. 4. Mass size distributions for PM mass obtained by the ELPI, SDI and DMPS-APS. The DMPS and APS mass size distributions are calculated with composite and gravimetric density. The sampling periods of (a) 7–9 May and (b) 26–28 May were selected because of distinct concentration levels and air mass types during these periods. The air masses originated from (a) south-east and (b) the Arctic Ocean.

ELPI, SDI, DMPS and APS. The raw concentration data provided by the SDI for each impactor stage were run through the inversion code MICRON (Wolfenbarger and Seinfeld 1990) to obtain the inverted mass size distribution. However, the mass concentrations of the SDI were too small in two cases for a proper extraction of the mass size distribution. For the DMPS-APS two different mass size distributions were calculated; one with the composite density and the other with the gravimetric density (densities shown in Table 4). For the ELPI only a single value of density (1.5 g cm^{-3}) was used, since the magnitude of density affects the mass concentrations of the ELPI by only a few percent. The last stage was excluded from the mass size distribution of the ELPI, since the ELPI was not able to measure the coarse size particle concentrations because of too small a number of particles in the background area.

Two examples of the mass size distribution of the ELPI, SDI and DMPS-APS are shown in Fig. 4. Although presented in separate graphs, the DMPS and APS results were considered as one mass size distribution.

The mass size distributions of the DMPS-APS and ELPI were quite similar, with one accumulation mode peaking at nearly the same size (Fig. 4). However, the mass size distribution of the SDI was slightly different. The SDI had two modes in the submicron size range, the dominant one peaking at around $0.5 \mu\text{m}$ and the

minor mode peaking at around $0.15 \mu\text{m}$. The minor mode of the SDI (at $0.15 \mu\text{m}$) was based on weighing results with large uncertainties due to small mass concentrations. Therefore, only the dominant mode in accumulation size range will be discussed in the subsequent sections. The dominant mode of the SDI was centered at larger particle size than that of the DMPS-APS and ELPI, but the mode was clearly smaller in magnitude than that of the DMPS-APS and ELPI. In the coarse size range the ELPI and the DMPS-APS had one mode and the SDI had one or two modes.

In order to study the accumulation mode in more detail, the mass median diameters (MMD) of the accumulation mode were calculated for the DMPS-APS and SDI for each sampling (Table 5). For two samplings the MMD of the SDI is missing because of small mass concentration and subsequent unsuccessful inversions. For the ELPI no continuous mass size distribution was available, and therefore the data of the ELPI is not presented in Table 5. The MMD of the SDI was larger than that of the DMPS-APS in all cases and the difference was greatest with the SDI and the DMPS-APS calculated using the composite density. On average the difference between the MMD of the SDI and DMPS-APS was 23% and 20% for the DMPS distribution calculated with composite and gravimetric density, respectively, as compared with the MMD of the SDI. This shift of the MMD was likely

caused by the difference in the relative humidity during the sampling, since the SDI mass size distribution was measured at ambient relative humidity while for the ELPI and DMPS the drier was used.

The SDI mass size distributions have quite a large uncertainty in weighing during small mass concentration periods. Since 30% of the PM_{10} mass was comprised of sulfate, which was accurately analyzed by IC, the sulfate of the SDI was assumed to mimic the mass size distribution of the SDI in accumulation size range. From the MMDs of the accumulation mode for the sulfate it can be seen that in some cases sulfate peaked at the same size as SDI mass, but in many cases sulfate peaked at smaller or larger particle size than mass (Table 5). The difference between the MMD of the SDI sulfate and that of the SDI mass was in the range 0.4%–22% with an average 9% and standard deviation of 9% as compared with that of the MMD of the SDI mass. The difference between the MMD of the sulfate and that of the DMPS-APS mass was quite similar to the corresponding value for the SDI mass and DMPS-APS mass with values of 23% and 18% for the DMPS-APS mass size distributions calculated with composite and gravimetric density, respectively, as compared with that for the MMD of sulfate. The relative humidity during the sampling can not completely explain the difference between the MMD of the sulfate and that of the DMPS. However, in the sampling when the relative humidity was the largest (18–20

May) the difference between the MMD of the sulfate and that of the DMPS-APS was the largest. Also, generally the MMD measured with the SDI is larger than the DMPS dry diameter. The contribution of the organic material to the MMD of the accumulation mode is difficult to assess, because of the lack of the accurate calibration of the SDI for quartz fiber substrates.

PM during nucleation events

The mass closure and PM_{10} experiments, presented in this paper, were carried out at the SMEAR II station, where aerosol formation and subsequent particle growth has been observed regularly (*see* Kulmala *et al.* 2001). Several nucleation events were detected also during the measurement campaign in May 2004, and due to the long sampling periods of two days or more, nearly all the periods had one or two nucleation events. Only the first two sampling periods (7–9 May and 9–11 May) and the ninth period (26–28 May) had clearly no nucleation events. The frequency of the events and the lack of those in the beginning of the measurement campaign, when the concentrations were elevated, are in accordance with the findings that nucleation in Hyytiälä is typically connected to clean Polar air masses (Kulmala *et al.* 2001).

In order to compare the chemical composition of the particles during the nucleation event periods with the respective composition during

Table 5. The modal mass median diameter (in μm) of the accumulation mode for mass (DMPS-APS, SDI) and sulfate (SDI).

Measurement period	Mass		Sulfate SDI
	DMPS-APS	SDI	
7–9 May 2004	0.383 ^a	0.420 ^b	0.468
9–11 May 2004	0.403 ^a	0.411 ^b	0.507
11–16 May 2004	0.323 ^a	0.324 ^b	0.413
16–18 May 2004	0.286 ^a	0.313 ^b	0.451
18–20 May 2004	0.235 ^a	0.235 ^b	0.355
20–22 May 2004	0.252 ^a	0.275 ^b	0.320
22–24 May 2004	0.321 ^a	0.363 ^b	0.291
24–26 May 2004	0.297 ^a	0.315 ^b	0.422
26–28 May 2004	0.359 ^a	0.413 ^b	0.489
28–31 May 2004	0.275 ^a	0.282 ^b	0.359

^a calculated with the composite density, ^b calculated with the gravimetric density.

the non-event periods, the sampling periods were divided into two cases: event and non-event samplings. Three different mass concentration levels (high, moderate and low) were observed in the non-event samplings, whereas the concentrations were always small when the nucleation events were detected. No clear conclusion from the OC/sulfate ratios in different particle size classes can be drawn, even though for the PM₁ (sum of stages 1–7) slightly larger OC/sulfate ratios were obtained for the event samples as compared with those for non-event samples (Table 6). Equally, the ratio of OC to ammonium and the ratio of sulfate to ammonium were calculated for the same samplings and size classes (not shown here), but no differences were found.

The lack of definite differences in the chemical composition between event samples and non-event samples may be due to the particle size range measured, since the SDI is not able to measure the particles below 0.05 μm , which is the size range most affected by aerosol formation by nucleation. Also, the time evolution of nucleation event cannot be seen in the impactor data due to the long integration time. The results of this study are in agreement with the work of Mäkelä *et al.* (2001). They collected event and non-event particles separately and analyzed them chemically, but found only small differences between the event and non-event sample sets. The most significant difference was found for dimethylammonium not analyzed in this work.

The MMD of sulfate peaks at smaller sizes in the event samples than in the non-event samples (Table 6). Comparing the non-event and event samples with small mass concentrations (26–28 May and 20–22 May), the shift in the MMD of the sulfate accumulation mode was as large as 0.2

μm (42% as compared with that of the non-event MMD). However, this shift might be due to the different air masses rather than due to the nucleation event. Also, the mass size distribution data of the SDI, ELPI and DMPS-APS were studied in order to find differences between event and non-event samples, but no such differences were found. Overall, the long sampling time used in this study is a severe limitation when nucleation events are investigated. The sample is not only a mixture of event and non-event particles but also a mixture of different air masses.

Summary and conclusions

A complete size-resolved chemical characterization of atmospheric aerosols was carried out at the forest station SMEAR II, in Finland, in May 2004. A total of ten samplings were conducted. Two 12-stage low pressure impactors and two virtual impactors were used in parallel in order to derive mass, ions, OC and EC of which the chemical mass closure was constructed. In addition to the impactors, size-segregated mass was also measured continuously with the ELPI, DMPS and APS. The focus of this study was on the fine size fraction (particle diameter < 1 μm).

In the beginning of the measurement campaign the concentrations of mass, ions, OC and EC were elevated. After that, the concentrations were small. The chemical composition of the particles was nearly constant during the measurement campaign with no clear differences between samples with large and small concentrations. The most prominent components in fine particles were ammonium sulfate (40%), OC (35%) and EC (5%). In most of the samples, the

Table 6. Comparison between the event and non-event samplings.

Measurement period	Status	OC/sulfate			MMD of sulfate (μm)
		Stage 1 (0.045–0.088 μm)	Stage 2 (0.088–0.142 μm)	Stages 1–7 (0.045–1.06 μm)	
7–9 May 2004	High conc. no event	3.13	1.18	0.85	0.480
9–11 May 2004	Moderate conc. no event	6.72	1.73	0.93	0.505
26–28 May 2004	Low conc. no event	4.88	2.12	1.10	0.500
20–22 May 2004	Low conc. event	8.05	3.87	1.58	0.292
24–26 May 2004	Low conc. event	3.87	1.36	1.24	0.330

size distributions of mass and ammonium sulfate were unimodal in the submicron size range with a mode peaking at 0.3–0.5 μm .

Nearly a complete chemical mass closure was reached for fine particles with only a slight difference between the chemical and gravimetric mass. On average the chemical to gravimetric mass ratio was 0.98 ± 0.10 and 1.05 ± 0.13 for the VI and the SDI, respectively. The most crucial part of the mass closure study was the weighing of the impactor substrates with small mass loading, which could result in uncertainties of 50% for individual impactor stages. Another uncertainty in the chemical mass closure study was the size distributions of OC and EC which were measured with a SDI loaded with quartz fiber substrates. Exact impactor collection efficiency curves for quartz fiber substrates were not available.

Quite a good agreement was obtained for the mass size distributions measured with the different types of instruments. The mass size distributions of the SDI and APS were measured at an ambient relative humidity, while those of the ELPI and the DMPS were measured using a drier. Because of that the maximum of the accumulation mode of the SDI was at larger particle size than that of the ELPI and the DMPS.

Semivolatile components may have been lost in the impactors, while the ELPI, DMPS and APS measured them due to immediate detection. That was observed when the total concentration of the accumulation mode (PM_1) was calculated for all the sampling periods. The PM_1 concentration of the ELPI was greater than that of the SDI and the reference sampler (VI) with an average ELPI to VI ratio of 1.11 ± 0.13 . The influences of semivolatile components on the DMPS-APS to VI mass concentration ratio could not be exactly quantified because the mass concentration of the DMPS-APS was calculated from the number concentration requiring an estimate for the particle density. The particle density was calculated in two different ways: from the chemical composition of particles and by comparing the mass obtained from the DMPS-APS combination with the VI mass concentration. On average the densities obtained in this study were 1.49 ± 0.03 and 1.66 ± 0.13 g cm^{-3} for the composite and gravimetric density, respectively, for the fine particles.

During the measurement campaign new-particle formation and subsequent growth of these particles were observed several times. The chemical composition of the nucleation event and non-event samples were compared, but no clear conclusion can be drawn from the results. The sampling period was two days or more and, therefore, the small differences between the nucleation event and non-event period were mixed with the differences between the different air masses. In a background environment, shortening the sampling time to one day or less is not possible with the impactor set-up used in this study. Therefore, detailed size- and time-resolved data on the chemical composition of the aerosol needed in analyzing nucleation events can be obtained only by on-line measurement systems.

Acknowledgements: The financial support from the Academy of Finland (contract no. 201131) is gratefully acknowledged.

References

- Brewer P.G. 1975. Minor elements in sea water. In: Chester R. (ed.), *Chemical oceanography*, vol. 1, Academic Press, San Diego, California, pp. 417–425.
- Chow J.C., Watson J.G., Fujita E.M., Lu Z., Lawson D.R. & Ashbaugh L.L. 1994. Temporal and spatial variations of $\text{PM}_{2.5}$ and PM_{10} in the southern California air quality study. *Atmos. Environ.* 28: 2061–2080.
- Fraser M.P., Yue Z.W., Tropp R.J., Kohl S.D. & Chow J.C. 2002. Molecular composition of organic fine particulate matter in Houston TX. *Atmos. Environ.* 36: 5751–5758.
- Gundel L.A., Lee V.C., Mahanama K.R.R., Stevens R.K. & Daisey J.M. 1995. Direct determination of the phase distributions of semi-volatile polycyclic aromatic hydrocarbons using annular denuders. *Atmos. Environ.* 29: 1719–1733.
- Harrison R.M., Jones A.M. & Lawrence R.G. 2003. A pragmatic mass closure model for airborne particulate matter at urban background and roadside sites. *Atmos. Environ.* 37: 4927–4933.
- Hinds W.C. 1999. *Aerosol technology: properties, behaviour, and measurement of airborne particles*, 2nd ed., John Wiley and Sons, New York.
- Hitzenberger R., Berner A., Galambos Z., Maenhaut W., Cafmeyer J., Schwarz J., Müller K., Spindler G., Wieprecht W., Acker K., Hillamo R. & Mäkelä T. 2004. Intercomparison of methods to measure the mass concentration of the atmospheric aerosol during INTERCOMP2000 — influence of instrumentations and size cuts. *Atmos. Environ.* 38: 6467–6476.
- Jokinen V. & Mäkelä J.M. 1997. Closed loop arrangement

- with critical orifice for DMA sheath/excess flow system. *J. Aerosol Sci.* 28: 643–648.
- Kulmala M., Hämeri K., Aalto P.P., Mäkelä J.M., Pirjola L., Nilsson E.D., Buzorius G., Rannik Ü., Dal Maso M., Seidl W., Hoffmann T., Janson R., Hansson H.-C., Viisanen Y., Laaksonen A. & O'Dowd C.D. 2001. Overview of the international project on biogenic aerosol formation in the boreal forest (BIOFOR). *Tellus* 53B: 324–343.
- Lonati G., Giugliano M., Butelli P., Romele L. & Tardivo R. 2005. Major components of PM_{2.5} in Milan (Italy). *Atmos. Environ.* 39: 1925–1934.
- Loo B.W. & Cork C.P. 1988. Development of high efficiency virtual impactor. *Aerosol Sci. Technol.* 9: 167–170.
- Maenhaut W., Hillamo R., Mäkelä T., Jaffrezo J.-L., Bergin M.H. & Davidson C.I. 1996. A new cascade impactor for aerosol sampling with subsequent PIXE analysis. *Nucl. Inst. Meth. Phys. Res. B* 109/110: 482–487.
- Mäkelä J.M., Aalto P., Jokinen V., Pohja T., Nissinen A., Palmroth S., Markkanen T., Seitsonen K., Lihavainen H. & Kulmala M. 1997. Observations of ultrafine particle formation and growth in boreal forest, *Geophys. Res. Lett.* 24: 1219–1222.
- Mäkelä J.M., Yli-Koivisto S., Hiltunen V., Seidl W., Swietlicki E., Teinilä K., Sillanpää M., Koponen I., Paatero J. & Rosman K. 2001. Chemical composition of aerosol during particle formation events in boreal forest. *Tellus* 53B: 380–393.
- Marjamäki M. & Keskinen J. 2004. Effect of impaction plate roughness and porosity on collection efficiency. *J. Aerosol Sci.* 35: 301–308.
- Matta E., Facchini M.C., Decesari S., Mircea M., Cavalli F., Fuzzi S., Putaud J.-P. & Dell'Acqua A. 2003. Mass closure on the chemical species in size-segregated atmospheric aerosol collected in an urban area of the Po Valley, Italy. *Atmos. Chem. Phys.* 3: 623–637.
- McMurry P.H., Wang X., Park K. & Ehara K. 2002. The relationship between mass and mobility for atmospheric particles: a new technique for measuring particle density. *Aerosol Sci. Technol.* 36: 227–238.
- Nuestüb C., Weise D., Birmili W., Wex H., Wiedensohler A. & Covert D.S. 2000. Size-segregated chemical, gravimetric and number distribution-derived mass closure of the aerosol in Sagres, Portugal during ACE-2. *Tellus* 52B: 169–184.
- Pakkanen T.A., Kerminen V.-M., Korhonen C.H., Hillamo R.E., Aarnio P., Koskentalo T. & Maenhaut W. 2001. Use of atmospheric elemental size distributions in estimating aerosol sources in the Helsinki area. *Atmos. Environ.* 35: 5537–5551.
- Putaud J.-P., Van Dingenen R., Dell'Acqua A., Raes F., Matta E., Decesari S., Facchini M.C. & Fuzzi S. 2004. Size-segregated aerosol mass closure and chemical composition in Monte Cimone (I) during MINATROC. *Atmos. Chem. Phys.* 4: 889–902.
- Putaud J.-P., van Dingenen R., Mangoni M., Virkkula A., Raes F., Maring H., Prospero J.M., Swietlicki E., Berg O.H., Hillamo R. & Mäkelä T. 2000. Chemical mass closure and assessment of the origin of the submicron aerosol in the marine boundary layer and the free troposphere at Tenerife during ACE-2. *Tellus* 52B: 141–168.
- Puxbaum H., Rendl J., Allabashi R., Otter L. & Scholes M.C. 2000. Mass balance of the atmospheric aerosol in a South African subtropical savanna (Nylsvley, May 1997). *J. Geophys. Res.* 105: 20697–20706.
- Radzi Bin Abas M., Rahman N.A., Omar N.Y.M.J., Jamil Maah M., Abu Samah A., Oros D.R., Otto A. & Simoneit B. 2004. Organic composition of aerosol particulate matter during a haze episode in Kuala Lumpur, Malaysia. *Atmos. Environ.* 38: 4223–4241.
- Rogge W.F., Mazurek M.A., Hildemann L.M., Cass G.R. & Simoneit B.R.T. 1993. Quantification of urban organic aerosols at a molecular level: identification, abundance and seasonal variation. *Atmos. Environ.* 27A: 1309–1330.
- Russel L.M. 2003. Aerosol organic-mass-to-organic-carbon ratio measurements. *Environ. Sci. Technol.* 37: 2982–2987.
- Salma I., Maenhaut W., Zemplén-Papp E. & Zárny G. 2001. Comprehensive characterization of atmospheric aerosols in Budapest, Hungary: physicochemical properties of inorganic species. *Atmos. Environ.* 35: 4367–4378.
- Seinfeld J.H. & Pandis S.N. 1998. *Atmospheric chemistry and physics: from air pollution to climate change*, John Wiley and Sons, New York.
- Sellegrri K., Laj P., Peron F., Dupuy R., Legrand M., Preunkert S., Putaud J.-P., Cachier H. & Ghermandi G. 2003. Mass balance of free tropospheric aerosol at the Puy de Dôme (France) in winter. *J. Geophys. Res.* 108, doi:10.1029/2002JD002747.
- Sillanpää M., Hillamo R., Mäkelä T., Pennanen A.S. & Salonen R. 2003. Field and laboratory tests of a high volume cascade impactor. *J. Aerosol Sci.* 34: 485–500.
- Stein S.W., Turpin B.J., Cai X., Huang P.-F. & McMurry P.H. 1994. Measurements of relative humidity-dependent bounce and density for atmospheric particles using the DMA-impactor technique. *Atmos. Environ.* 28: 1739–1746.
- Stohl A. & Wotawa G. 1995. A method for computing single trajectories representing boundary layer transport. *Atmos. Environ.* 29: 3235–3239.
- Teinilä K., Kerminen V.-M. & Hillamo R. 2000. A study of size-segregated aerosol chemistry in the Antarctic atmosphere. *J. Geophys. Res.* 105: 3893–3904.
- Temesi D., Molnár A., Mészáros E., Feczko F., Gelencsér A., Kiss G. & Krivácsy Z. 2001. Size-resolved chemical mass balance of aerosol particles over rural Hungary. *Atmos. Environ.* 35: 4347–4355.
- Tolocka M.P., Solomon P.A., Mitchell W., Norris G.A., Gemmill D.B., Wiener R.W., Vanderpool R.W., Homolya J.B. & Rice J. 2001. East versus West in the US: Chemical Characteristics of PM_{2.5} during the Winter of 1999. *Aerosol Sci. Technol.* 34: 88–96.
- Turpin B.J. & Lim H.-J. 2001. Species contributions to PM_{2.5} mass concentrations: revisiting common assumptions for estimating organic mass. *Aerosol Sci. Technol.* 35: 602–610.
- Turpin B.J., Saxena P. & Andrews E. 2000. Measuring and simulating particulate organics in the atmosphere: problems and prospects. *Atmos. Environ.* 34: 2983–3013.
- Viidanoja J., Kerminen V.-M. & Hillamo R. 2002. Measuring

the size distribution of atmospheric organic and black carbon using impactor sampling coupled with thermal carbon analysis: method development and uncertainties. *Aerosol Sci. Technol.* 36: 1–10.

Winklmayr W., Reischl G.P., Lindner A.O. & Berner A. 1991.

A new electromobility spectrometer for the measurement of aerosol size distribution in the size range from 1 to 1000 nm. *J. Aerosol Sci.* 22: 289–296.

Wolfenbarger J.K. & Seinfeld J.H. 1990. Inversion of aerosol size distribution data. *J. Aerosol Sci.* 21: 227–247.

Received 26 April 2005, accepted 1 August 2005

Appendix

Uncertainty budget for the mass closure

The variance $S(y)^2$ may be approximated according to the law of propagation of errors by:

$$S(y)^2 = \left(\frac{df}{dx_1}\right)^2 S(x_1)^2 + \left(\frac{df}{dx_2}\right)^2 S(x_2)^2 + \dots + \left(\frac{df}{dx_n}\right)^2 S(x_n)^2 \quad (\text{A1})$$

where $y = f(x_1, x_2, \dots, x_n)$ is a function of n non-correlated parameters (x_1, x_2, \dots, x_n) . (df/dx_i) represents the partial derivative of f with respect to x_i applied to (x_1, x_2, \dots, x_n) , and $S(x_i)$ is the uncertainty of parameter x_i (Putaud *et al.* 2000).

Gravimetric mass

Equation A1 was used to calculate the uncertainty of the gravimetric mass (Table 3) for the average sample by combining the random errors in the parameters and using average parameter values. The overall uncertainty was assessed to be due to the uncertainty in weighing, blank variability and the uncertainty in sampling air volume.

Chemical mass

Equation A1 was also used to calculate the uncertainty of different chemical components associated with the chemical mass (Table 3). The overall uncertainty of each chemical component was assessed to be due to the analytical accuracy, blank variability, the uncertainty in sampling air volume and the uncertainty in OM/OC correction factor (only for OM). The sampling artifacts were excluded from the calculations due to difficulties in combining negative and positive artifacts. The overall uncertainty of the chemical mass was assessed by combining the relative uncertainties of chemical components according to the Eq. A1.

ELPI

The only parameter that was used for assessing the uncertainty of the ELPI results was density. In calculations the density of 1.5 g cm^{-3} was used. The uncertainty due to the uncertainty in density was estimated to be -1.7% , 3.0% (corresponding uncertainty in density of $-0.5, 0.3 \text{ g cm}^{-3}$). The uncertainty in the current measurement is about 5 fA corresponding to 5%–10% uncertainty in the accumulation mode mass concentration during 11–30 May and lower uncertainties for higher concentrations during 7–11 May.

DMPS

Data has been verified against the condensation particle counters (TSI3025 and TSI3010) using integrated total number concentration of the DMPS. The agreement was better than 10%. Parameters that have been taken into account in concentration calculations are diffusion losses in the sampling line (0.5 m), charge distribution, transfer functions, losses inside the DMA and TSI3025 and TSI3010 losses.

APS

There were no coincidence errors during the measurement period. This can be seen directly from the data of the APS using the double-crested signal processing technique. The detection efficiency of the APS below $0.6 \mu\text{m}$ (aerodynamic diameter) is obviously below 100% (*see* Fig. 4). Therefore the PM_{10} concentration for the DMPS-APS combination is based on the DMPS data until $0.67 \mu\text{m}$ (aerodynamic diameter).